

Relativistic Precession of Quantum Elliptical States in the Coulomb Potential

Michael G.A. Crawford
 Laboratory of Atomic and Solid State Physics,
 Cornell University, Ithaca, NY, 14853-2501

January 9, 2001

Abstract

A special relativistic perturbation to non-relativistic quantum mechanics is shown to lead to the special relativistic prediction for the rate of precession for quantum states in the Coulomb potential. This behavior is shown using $SO(4)$ coherent states as examples. These states are localized on Kepler ellipses and precess in the presence of a relativistic perturbation.

1 Introduction

It is well known that the precession of the perihelion of Mercury's orbit is an important experimental test of general relativity. The total rate of precession is 574 arcseconds per century, all but about 43 of which (5×10^{-7} rad/period) may be accounted for by Newtonian perturbation [1]. A general relativistic calculation was first accomplished by Einstein in 1915, and a modern treatment with accurate values for the relevant constants gives 42.98 arcseconds per century [2, 3]. Clearly, general relativity passes this test, although some authors argue that contributions to the precession due to the solar quadrupole moment has been understated [4].

A similar calculation may be carried out in the context of special relativity, a calculation which dates back at least as far as 1921 by Sommerfeld [5]. In the context of calculating the fine structure of the hydrogen atomic spectrum in the old quantum theory, Sommerfeld calculated the classical rate of precession due to a special relativistic treatment of the kinetic energy of a "spinless" electron in the Coulomb potential. This calculation yielded a rate of precession which is diminished from the general relativistic rate by a factor of six, confirming that special relativity does not give a complete treatment of relativistic effects. (Sommerfeld's calculation ignored electron spin in part because it was not described until 1925 by Uhlenbeck and Goudsmit.)

Nonetheless, turning to quantum mechanics, relativistic effects may be partially incorporated into non-relativistic behavior through a perturbation to kinetic energy motivated by special relativistic considerations. (The rest originates from spin-orbit coupling, presently ignored.) Therefore, when making comparisons between classical and quantum calculations, the relativistic quantum mechanical calculation aught to be compared to the special relativistic calculation, even though the general relativistic calculation is likely closer to the truth.

With the fine structure representing the most obvious quantum mechanical appearance of relativistic effects, and precession of orbits representing an important classical manifestation of relativistic effects, the question arises, may one of these be described in terms of the other? As shown below, the classical special relativistic prediction is recovered from a quantum prediction derived through a special relativistic perturbation to non-relativistic quantum mechanics.

In order to carry through the calculations of these estimates, one requires a few assumptions regarding the quantum wave functions under consideration. In order to test these assumptions, there exist the $SO(4)$ coherent states. These states, generalizations of the standard harmonic oscillator coherent states [6], are

quantum in description yet localized around the classical, elliptical orbits [7]. After testing for the assumptions mentioned above, a sample state may be evolved to ascertain whether or not the calculated estimates are borne out under quantum evolution.

2 Estimating the rate of precession

For the initial considerations, one requires the hydrogenic spectrum and the first order correction to the energy from Raleigh-Schrödinger perturbation theory due to the perturbation to kinetic energy. From any standard text on quantum mechanics [8] the energy eigenlevels of the Hamiltonian

$$\hat{H}_0 = \frac{p^2}{2m} - \frac{Ze^2}{r} \quad (1)$$

are given by

$$E_n^{(0)} = -\frac{mZ^2e^4}{2\hbar^2n^2}, \quad (2)$$

and the first order Raleigh-Schrödinger perturbative correction to this Hamiltonian due to the perturbation

$$\hat{H}_1 = -\frac{p^4}{8m^3c^2} \quad (3)$$

is given by

$$E_{n,\ell}^{(1)} = -\frac{mZ^4e^8}{2\hbar^4c^2n^3} \left(\frac{1}{\ell + \frac{1}{2}} - \frac{3}{4n} \right), \quad (4)$$

in which m is the electron mass, Z is the atomic number, e is the electron charge, c is the speed of light, n is the total quantum number, and ℓ is the quantum number pertaining to total angular momentum, the eigenvalues of \hat{L}^2 given by $\hbar^2\ell(\ell + 1)$. The perturbation Eq. (3) is obtained by expanding the special relativistic expression for the kinetic energy and retaining the next term after the standard Newtonian term.

Following along similar lines as those in describing wave function revivals [9, 10, 11, 12], the classical period may be extracted from the spectrum Eq. (2). For the purposes of this calculation, assume that the system is in some state $|\psi\rangle$ with average total quantum number $\langle n \rangle$ and uncertainty Δn . Expanding the energy eigenlevels about $n = \langle n \rangle$,

$$E_n^{(0)} = -\frac{mZ^2e^4}{2\hbar^2} \left(\frac{1}{\langle n \rangle^2} + \frac{2}{\langle n \rangle^3}(n - \langle n \rangle) - \frac{3}{\langle n \rangle^4}(n - \langle n \rangle)^2 + O((n - \langle n \rangle)^3) \right). \quad (5)$$

If one expresses the quantum time evolution of the state in terms of the eigenstate expansion,

$$|\psi(t)\rangle = \sum_n e^{-iE_n t/\hbar} c_n |n\rangle, \quad (6)$$

the first term leads to an overall phase factor which may be dropped. The second term will lead to phase factors that are integer multiples of 2π when

$$\frac{mZ^2e^4}{\hbar^2\langle n \rangle^3} T_{cl}/\hbar = 2\pi \quad (7)$$

or

$$T_{cl} = \frac{2\pi\hbar^3\langle n \rangle^3}{mZ^2e^4}. \quad (8)$$

This gives the classical period of a classical trajectory with energy E_n^0 exactly, a circumstance closely connected to the success of Bohr-Sommerfeld quantization in hydrogenic atoms. Also, for hydrogenic wave functions, radial expectation values are given by

$$r_n = \langle n, \ell, m | \hat{r} | n, \ell, m \rangle = \frac{n^2 \hbar^2}{Z m e^2}. \quad (9)$$

Substitution of this value into T_{cl} yields

$$T_{cl}^2 = \frac{4\pi^2 r_n^3}{Z^4 e^4}, \quad (10)$$

a quantum approach, if you will, to Kepler's third law.

Thus, the linear term in Eq. (5) contributes integer multiples of 2π in phase at $t = T_{cl}$. If this were all, the state at $t = T_{cl}$ would equal the original (up to an overall phase factor). This is not all: The quadratic contribution provides a "dephasing" influence. If this contribution is small, the state at $t = T_{cl}$ will closely resemble the original state. Evaluating the quadratic contribution at the edge of the distribution in n ($n = \langle n \rangle + \Delta n$) at $t = T_{cl}$ yields the "test quantity"

$$\delta\phi = 3\pi \frac{(\Delta n)^2}{\langle n \rangle}. \quad (11)$$

If $\delta\phi \ll 2\pi$, after one classical period, the state approximately reassembles its initial self. In the special case of a state localized in position and momentum, Ehrenfest's equations indicate an initial trajectory which follows a classical trajectory. In the additional case that $\delta\phi$ is small, the state achieves at least a full period of behavior approximating classical behavior.

Now treating the relativistic perturbation to kinetic energy Eq. (4), suppose the system is now in a state composed of eigenstates pertaining to the same n , degenerate in the unperturbed system. Then, the expansion about $\ell = \langle \ell \rangle$ of the perturbation Eq. (4) is given by

$$E_{n,\ell}^{(1)} = \frac{mZ^4 e^8}{2\hbar^4 c^2 n^3} \left[-\left(\frac{1}{\langle \ell \rangle + \frac{1}{2}} - \frac{3}{4n} \right) + \frac{(\ell - \langle \ell \rangle)}{(\langle \ell \rangle + \frac{1}{2})^2} - \frac{(\ell - \langle \ell \rangle)^2}{(\langle \ell \rangle + \frac{1}{2})^3} + O((\ell - \langle \ell \rangle)^3) \right]. \quad (12)$$

Consistent with the argument that a perturbative approach to calculating energy levels is appropriate, the value of $E_{n,\ell}^{(1)}$ is small compared to $E_n^{(0)}$, so that time evolution due to $E_{n,\ell}^{(1)}$ will be slow on the scale of T_{cl} . Indeed, following the calculation of T_{cl} above, the term independent of $(\ell - \langle \ell \rangle)$ of Eq. (12) leads to overall phase factors, and the linear term leads to integer multiples of 2π when

$$\frac{mZ^4 e^8}{2\hbar^4 c^2 n^3} \frac{1}{(\langle \ell \rangle + \frac{1}{2})^2} \frac{T_p}{\hbar} = 2\pi \quad (13)$$

or

$$T_p = \frac{4\pi\hbar^5 c^2 n^3}{mZ^4 e^8} \left(\langle \ell \rangle + \frac{1}{2} \right)^2. \quad (14)$$

This may be written in terms of T_{cl} , yielding

$$T_p = \frac{2\hbar^2 c^2}{Z^2 e^4} T_{cl} \left(\langle \ell \rangle + \frac{1}{2} \right)^2. \quad (15)$$

Continuing the analogous arguments which lead to Eq. (11), the quadratic term of Eq. (12) evaluated at $t = T_p$ at the edges of the distribution in ℓ yields the test parameter

$$\delta\phi = \frac{1}{2} \frac{mZ^4 e^8 (\Delta\ell)^2}{\hbar^4 c^2 n^3 (\langle \ell \rangle + \frac{1}{2})^3} \frac{T_p}{\hbar} = \frac{2\pi(\Delta\ell)^2}{\langle \ell \rangle + \frac{1}{2}}. \quad (16)$$

Hence, if $\delta\phi$ is small, then the state at $t = T_p$ will approximately resemble the state at $t = 0$.

From Will [3], the classical rate of perihelion precession according to a general relativistic calculation is given by

$$\delta\omega = 6\pi \frac{G^2 M^2 m^2}{c^2 L^2}, \quad (17)$$

measured as a change in angle per classical period of the vector pointing from perihelion to aphelion. In this expression, G is the gravitational constant, M is the (large) mass of the source of the gravitational field, m is the (small) mass of body in orbit, and L is the orbital angular momentum of the orbiting body. The special relativistic calculation of the rate of precession is (from Bergmann [13])

$$\delta\omega = \pi \frac{G^2 M^2 m^2}{c^2 L^2}. \quad (18)$$

As mentioned earlier, special relativity is not a complete relativistic description of space; the general relativistic calculation is the correct one, agreeing with the observed precession of Mercury. Using the relation

$$\frac{\delta\omega}{2\pi} = \frac{T_{cl}}{T_p}, \quad (19)$$

the quantum prediction of the same measurement is given by, from Eq. (15),

$$\delta\omega = \frac{\pi Z^2 e^4}{c^2 \hbar^2 (\langle \ell \rangle + \frac{1}{2})^2}. \quad (20)$$

To compare this rate with the astrophysical calculations, replace the strength of the Coulomb potential (Ze^2) with that of the Kepler problem (GMm), and note that the total angular momentum squared will be close to $\hbar^2(\langle \ell \rangle + \frac{1}{2})^2$ given the above assumptions that $\langle \ell \rangle$ is large and $(\Delta\ell)^2$ is small:

$$\langle \ell(\ell + 1) \rangle - (\langle \ell \rangle + \frac{1}{2})^2 = (\Delta\ell)^2 - \frac{1}{4}. \quad (21)$$

These substitutions yield for the quantum estimate of the rate of precession

$$\delta\omega = \pi \frac{G^2 M^2 m^2}{c^2 L^2}, \quad (22)$$

in complete agreement with the special relativistic estimate as anticipated. This agreement remains after two first order approximations: one through the perturbative approach leading to Eq. (4), and the other in the expansion of Eq. (4) about $\ell = \langle \ell \rangle$.

3 SO(4) coherent states

The useful coherent states in this context are those developed by Perelomov [14, 15] as generalizations of the standard coherent states for the harmonic oscillator [6]. This generalization rests upon the group structure of the system in question. In the case of the hydrogen atom, the dynamical group is SO(4,2) [16, 17]. For a pedagogical review, see Adams *et al.* [18]. For the present purposes, it is not necessary to engage the entire group; one only requires the degeneracy group SO(4). Treatments of coherent states of this description are existent in the literature [7, 12].

The realization of SO(4) which describes the degeneracy of the hydrogen atom spectrum is given by the elements of the angular momentum operator and those of the scaled Laplace-Runge-Lenz vector. The classical version of the Laplace-Runge-Lenz vector is proportional in magnitude to the eccentricity of the

orbit in question, aligned parallel to the major axis. The corresponding quantum operators in atomic units are given by [18]

$$\hat{\mathbf{L}} = \hat{\mathbf{r}} \times \hat{\mathbf{p}}, \quad (23)$$

$$\hat{\mathbf{A}} = \frac{1}{2} \hat{\mathbf{r}} \hat{p}^2 - \hat{\mathbf{p}}(\hat{\mathbf{r}} \cdot \hat{\mathbf{p}}) - \frac{1}{2} \hat{\mathbf{r}}. \quad (24)$$

All of these operators commute with the Hamiltonian, leading to conservation of these quantities under time evolution. Conservation of angular momentum is to be expected in this (spherically symmetric) potential, but conservation of the latter (a simple derivation of which is given by Wulfman [19]) is a unique property of the non-relativistic Coulomb potential. The classical interpretation of the constancy of the Laplace-Runge-Lenz vector is that elliptical orbits do not precess.

These operators satisfy the commutation relations

$$[\hat{L}_j, \hat{L}_k] = i\epsilon_{jkl} \hat{L}_l, \quad [\hat{A}_j, \hat{A}_k] = i\epsilon_{jkl} \hat{L}_l, \quad [\hat{L}_j, \hat{A}_k] = i\epsilon_{jkl} \hat{A}_l. \quad (25)$$

These six operators may be decoupled into two groups of three operators via

$$\hat{M}_j = \frac{1}{2}(\hat{L}_j + \hat{A}_j), \quad \hat{N}_j = \frac{1}{2}(\hat{L}_j - \hat{A}_j), \quad (26)$$

which commute according to

$$[\hat{M}_j, \hat{M}_k] = i\epsilon_{jkl} \hat{M}_l, \quad [\hat{N}_j, \hat{N}_k] = i\epsilon_{jkl} \hat{N}_l, \quad [\hat{M}_j, \hat{N}_k] = 0. \quad (27)$$

In terms of these new operators, it is clear that $\text{SO}(4) = \text{SO}(3) \otimes \text{SO}(3)$.

The group $\text{SO}(4)$ has two Casimir operators, given by

$$\hat{C}_1 = \hat{L}^2 + \hat{A}^2 = 2(\hat{M}^2 + \hat{N}^2), \quad (28)$$

$$\hat{C}_2 = \hat{\mathbf{L}} \cdot \hat{\mathbf{A}} = \hat{M}^2 - \hat{N}^2. \quad (29)$$

In the hydrogenic realization of this group, $\hat{C}_2 = 0$ so that quantum mechanically and classically, angular momentum is perpendicular to the Laplace-Runge-Lenz vector. The second Casimir operator also indicates that the dimensions of the irreducible representations of the $\text{SO}(3)$ generated by the \hat{M}_k and by the \hat{N}_k are equal (say, to $n = 2j + 1$) so that the dimensions of the relevant unitary irreducible representations of $\text{SO}(4)$ are n^2 , the famous degeneracy of the hydrogen atom energy spectrum. With this in mind, the first Casimir operator is equal to

$$\hat{C}_1 = 4j(j+1) = n^2 - 1, \quad (30)$$

representing a constraint on the sum $(\hat{L}^2 + \hat{A}^2)$.

Turning to the $\text{SO}(4)$ coherent states, the reader is referred to the references for details omitted in the following [6, 15, 20]. Since $\text{SO}(4) = \text{SO}(3) \otimes \text{SO}(3)$, the $\text{SO}(4)$ coherent states may be expressed as the direct product of two $\text{SO}(3)$ coherent states which are themselves standard in the literature. The $\text{SO}(3)$ coherent states are given by

$$|j, \zeta\rangle = \sum_{m=-j}^j \left(\frac{(2j)!}{(j+m)!(j-m)!} \right)^{1/2} \frac{\zeta^{j+m}}{(1+|\zeta|^2)^j} |j, m\rangle, \quad (31)$$

parameterized by the complex valued ζ . In these states, expectation values of the angular momentum operators are given by

$$\langle \hat{\mathbf{J}} \rangle = \frac{2j}{1+|\zeta|^2} \left(\text{Re}(\zeta), -\text{Im}(\zeta), \frac{1}{2}(|\zeta|^2 - 1) \right), \quad (32)$$

with $\hat{\mathbf{J}}$ standing for $\hat{\mathbf{M}}$ or $\hat{\mathbf{N}}$ as the case may be. With these expressions in mind, the $\text{SO}(4)$ coherent states are given by

$$|n, \zeta_1, \zeta_2\rangle = |j, \zeta_1\rangle |j, \zeta_2\rangle. \quad (33)$$

Here, $n = 2j + 1$, and ζ_1 and ζ_2 parameterize the SO(3) coherent states pertaining to $\hat{\mathbf{M}}$ and $\hat{\mathbf{N}}$ respectively. The expectation values of the angular momentum and Laplace-Runge-Lenz operators may be regained through Eq. (32) and the relations $\hat{\mathbf{L}} = \hat{\mathbf{M}} + \hat{\mathbf{N}}$ and $\hat{\mathbf{A}} = \hat{\mathbf{M}} - \hat{\mathbf{N}}$. In practice, to calculate examples of the SO(4) coherent states, Eq. (33) leads to the direct product states $|j, m_1\rangle|j, m_2\rangle$. Such states may be related to the standard hydrogenic eigenstates $|n, \ell, m\rangle$ via the Clebsch-Gordon coefficients.

For the purpose of visualization, spherical symmetry permits setting $\langle \hat{\mathbf{L}} \rangle$ parallel to the z -axis and $\langle \hat{\mathbf{A}} \rangle$ parallel to the x -axis. The former is accomplished by taking $\zeta_2 = -\zeta_1$, and the latter follows through $\text{Im}(\zeta_2) = \text{Im}(\zeta_1) = 0$. These identifications reduce the problem to the variation of a single real parameter, say $\eta = \text{Re}(\zeta_1)$. In terms of this parameter, expectation values are given by

$$\langle \hat{L}_3 \rangle = \frac{2j(\eta^2 - 1)}{1 + \eta^2}, \quad \langle \hat{A}_1 \rangle = \frac{4j\eta}{1 + \eta^2}. \quad (34)$$

Classically, the magnitude of the Laplace-Runge-Lenz vector is proportional to the eccentricity of the orbit in question. Taking ϵ to be the eccentricity of the classical orbit which underlies the quantum state, one finds that

$$\epsilon = \frac{2\eta}{1 + \eta^2}. \quad (35)$$

Also in terms of η , the total angular momentum may be expressed as

$$\langle \hat{L}^2 \rangle = 2j(j+1) + 2j^2 \frac{\eta^4 - 6\eta^2 + 1}{(1 + \eta^2)^2}. \quad (36)$$

This expression follows from $\langle \hat{L}^2 \rangle = \langle (\hat{\mathbf{M}} + \hat{\mathbf{N}}) \cdot (\hat{\mathbf{M}} + \hat{\mathbf{N}}) \rangle$, Eq. (32), and $\langle \hat{\mathbf{M}} \cdot \hat{\mathbf{N}} \rangle = \langle \hat{\mathbf{M}} \rangle \cdot \langle \hat{\mathbf{N}} \rangle$, the last of which since $[\hat{M}_j, \hat{N}_k] = 0$.

Note that the SO(4) coherent states are constructed so as to have minimal fluctuations about the appropriately rotated 4-dimensional angular momentum operators. This carries through to minimal fluctuations about the 3-dimensional angular momentum operators and the quantum Laplace-Runge-Lenz vector. One therefore expects the quantum SO(4) state to exhibit minimal fluctuations about an analogous classical orbit. Hence, given a value of η , the approximate geometry is given by Eq. (35), with a semi-major axis given by Eq. (9).

4 Precessing Coherent States

The value of the test parameter $\delta\phi$ given by Eq. (16) is expressible in closed form for these SO(4) coherent states. Recall that with expectation values taken in an SO(3) coherent state,

$$(\Delta \hat{J}_3)^2 = 2j \frac{\eta^2}{(1 + \eta^2)^2}, \quad (37)$$

and that

$$(\Delta \ell)^2 = (\Delta \hat{L}_3)^2 = (\Delta \hat{M}_3)^2 + (\Delta \hat{N}_3)^2, \quad (38)$$

since \hat{M}_j and \hat{N}_j commute. With these in mind, and dropping the $\frac{1}{2}$ from the denominator of $\delta\phi$ since $\langle \ell \rangle$ is large, one finds

$$\delta\phi = 2\pi \frac{\eta^2}{\eta^4 - 1}. \quad (39)$$

Clearly, the precession is in some sense the best $\eta = 0$ or as $\eta \rightarrow \infty$, but in either case, the precession will not be observed since, from Eq. (35), the eccentricity will be nil: There is a certain tradeoff between the observability and ‘‘coherence’’ of the precession measured by $\delta\phi$. In fact, it is convenient to express $\delta\phi$ in terms of ϵ from Eq. (35) so as to connect this test with a more physical or geometrical quantity:

$$\delta\phi = \frac{2\pi\epsilon^2(2 - \epsilon^2 \pm 2\sqrt{1 - \epsilon^2})}{8 - 8\epsilon^2 \pm 4(2 - \epsilon^2)\sqrt{1 - \epsilon^2}}. \quad (40)$$

(In this expression, the positive sign is appropriate for $\eta > 1$ and the negative for $\eta < 1$.) Plotting this expression in Figure 2, one sees that as the eccentricity increases, the degree to which the wave functions remain assembled decreases.

For some examples of precessing coherent states, examine Figure 3. This figure depicts a mesh plot of an $SO(4)$ coherent state at $t = 0$, and a series of overlayed contour plots showing states precessed from $t = 0$ to $t = \frac{1}{4}T_p$. To appreciate the physical scale of these simulations, the field of view in all cases is $4.23 \mu\text{m}$ across and with states in the 141st energy level, the classical period is 4.25×10^{-10} seconds. In Figure 3(b), with $\epsilon = 0.385$, the precession period is 0.266 seconds or 6.26×10^8 classical periods, which on atomic scales, is a very long time. In the subsequent images, the rate of precession is larger owing to the larger eccentricity such that the precession period of the state depicted in Figure 3(d) is 0.164 seconds, still an epoch in atomic terms.

As apparent from the images, the rate of precession is good agreement with the special relativistic prediction. In the case of Figure 3(b), though only shown until $t = \frac{1}{4}T_p$, the state remains localized on the ellipse up to the full period of the precession. Not surprisingly, for increased eccentricities, the degree of “coherence” of the state decreases, leading to the decay of the state as depicted in Figure 3(d) after only a quarter precession period.

5 Conclusions

An important point to be noted about the precession of these states is that the rate is neither the correct general relativistic rate as observed in the case of Mercury, nor the correct rate for an atomic system since the present treatment ignores spin orbit coupling. The present effort, however, is not oriented towards making a physical prediction to be tested in the laboratory. The purpose has been to show that a simple analysis of a quantum perturbation can reproduce the results of a more involved classical analysis. In particular, a special relativistic perturbation to non-relativistic quantum mechanics leads to an agreement with classical special relativity in a large quantum number limit. A similar notion of agreement may be found in the work of McRae and Vrscay [21] who have studied correspondence between quantum and classical perturbation schemes. In their work, as well as in the present paper, it transpires that the simplest route to the determination of a classical perturbation may be through the classical limit of a quantum perturbation.

Planetary extrapolations of quantum mechanics (which include, for example, the observation that the earth is at about the 2.5×10^{74} th eigenlevel of the sun-earth system) are often found in papers, especially those dealing with hydrogenic coherent states [22, 23, 24]. Such extrapolations are useful for considering the large scale implications of trends observed deep in the quantum regime. With the present considerations in mind, the special relativistic perturbation, which correctly accounts for part of the hydrogenic fine structure, generates the incorrect rate of precession for a planetary body. This theory gives a rate of precession for Mercury amounting to only 7.2 arcseconds per century. This failure, in principle, is no surprise: to do any better from a quantum mechanical starting point would likely require quantum gravity.

References

- [1] C.M. Will. *Was Einstein Right? Putting General Relativity to the Test*. BasicBooks, New York, 1993.
- [2] A.M. Nobili and C.M. Will. The real value of Mercury’s perihelion advance. *Nature*, 360:39–41, 1986.
- [3] C.M. Will. *Theory and Experiment in Gravitational Physics*. Cambridge University Press, Cambridge, revised edition, 1993.
- [4] T.J. Lydon and S. Sofia. A measurement of the shape of the solar disk: The solar quadrupole moment, the solar octopole moment, and the advance of the perihelion of Mercury. *Phys. Rev. Lett.*, 76(2):177–179, 1996.

- [5] A. Sommerfeld. *Atombau und Spektrallinien*. F. Vieweg und Sohn, Braunschweig, Germany, 1921.
- [6] J.R. Klauder and B.-S. Skagerstam, editors. *Coherent States: Applications in Physics and Mathematical Physics*. World Scientific, Singapore, 1985.
- [7] J.C. Gay, D. Delande, and A. Bommier. Atomic quantum states with maximum localization of classical elliptical orbits. *Phys. Rev. A*, 39(12):6587–6590, 1989.
- [8] J.S. Townsend. *A Modern Approach to Quantum Mechanics*. McGraw-Hill, Inc., New York, 1992.
- [9] I.S. Averbukh and N.F. Perelman. Fractional revivals: Universality in the long-term evolution of quantum wave packets beyond the correspondence principle dynamics. *Phys. Lett. A*, 139(9):449–453, 1989.
- [10] M. Nauenberg. Autocorrelation function and quantum recurrence of wavepackets. *J. Phys. B*, 23:L385–L390, 1990.
- [11] J.A. Yeazell, M. Mallalieu, and Jr. C.R. Stroud. Observation of the collapse and revival of a Rydberg electronic wave packet. *Phys. Rev. Lett.*, 64(17):2007–2010, 1990.
- [12] M.G.A. Crawford. Temporally stable coherent states in energy degenerate systems: The hydrogen atom. *Phys. Rev. A*, 62(1):012104–1–7, 2000.
- [13] G. Bergmann. *Introduction to the Theory of Relativity*. Prentice-Hall, Englewood Cliffs, NJ, 1942.
- [14] A.M. Perelomov. Coherent states for arbitrary Lie groups. *Commun. Math. Phys.*, 26:222–236, 1972.
- [15] A.M. Perelomov. *Generalized Coherent States and Their Applications*. Springer-Verlag, London, 1986.
- [16] A.O. Barut and G.L. Bornzin. SO(4,2)-Formulation of the symmetry braking in relativistic Kepler problems with or without magnetic charges. *J. Math. Phys.*, 12(5):841–846, 1971.
- [17] J. Paldus. Dynamical groups. In G. W. F. Drake, editor, *Atomic, Molecular and Optical Physics Handbook*. AIP Press, Woodbury, New York, 1996.
- [18] B.G. Adams, J. Čížek, and J. Paldus. Lie algebraic methods and their applications to simple quantum systems. In *Advances in Quantum Chemistry*, Vol 19. Academic Press, New York, 1988.
- [19] C.E. Wulfman. Dynamical groups in atomic and molecular physics. In E. M. Loeb, editor, *Group Theory and Its Applications*, volume II. Academic Press, New York, 1971.
- [20] W.-M. Zhang, D.H. Feng, and R. Gilmore. Coherent states: Theory and some applications. *Rev. Mod. Phys.*, 62(4):867–927, 1990.
- [21] S.M. McRae and E.R. Vrscay. Perturbation theory and the classical limit of quantum mechanics. *J. Math. Phys.*, 38(6):2899, 1997.
- [22] L.M. Brown. Classical limit of the hydrogen atom. *Am. J. Phys.*, 41:525, 1973.
- [23] R.F. Fox. Generalized coherent states. *Phys. Rev. A*, 59(5):3241–3255, 1999.
- [24] D. Bhaumik, B. Dutta-Roy, and G. Ghosh. Classical limit of the hydrogen atom. *J. Phys. A*, 19:1355–1364, 1986.

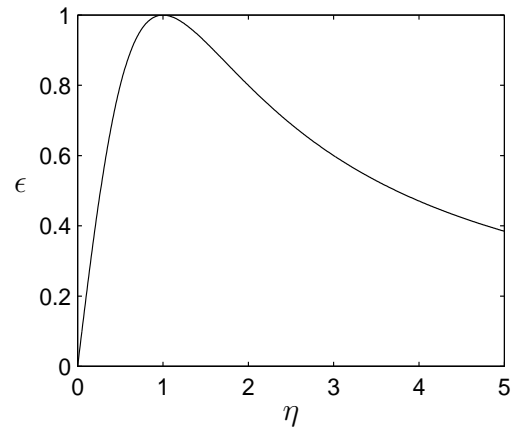


Figure 1: Eccentricity ϵ versus η , the parameter to the $SO(4)$ coherent state.

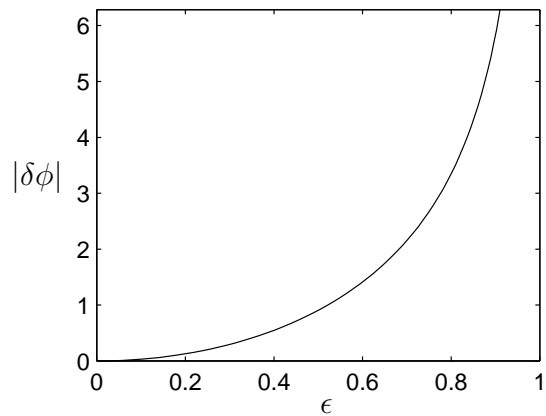


Figure 2: Test parameter $\delta\phi$ versus eccentricity ϵ .

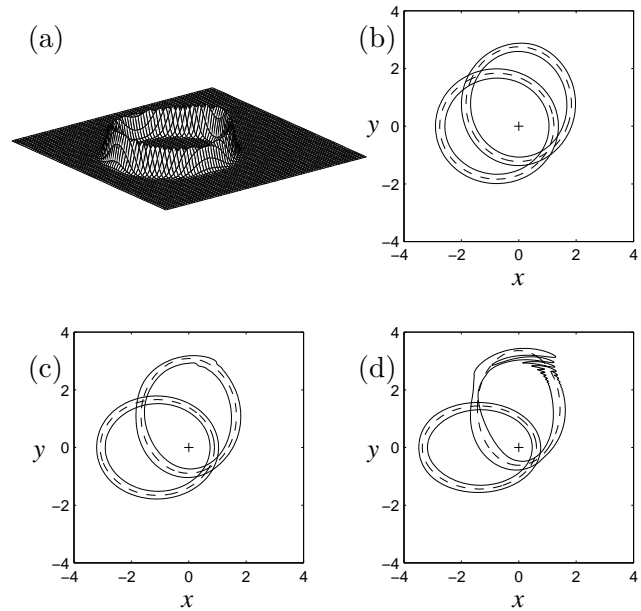


Figure 3: Some examples of precessing $SO(4)$ coherent states: (a) In the 141st energy level, at $t = 0$, with $\eta = 0.2$ (or $\epsilon = 0.385$) on the x - y plane with amplitude proportional to $|\langle \mathbf{r}|141, \zeta_1, \zeta_2 \rangle|^2$. Position is plotted in 10^4 atomic units, and the origin is located at the + symbol. (b) The same state as (a) on the same field, $t = 0$ oriented horizontally, and $t = \frac{1}{4}T_p$ oriented vertically. The solid lines depict a single contour on the quantum wave function, and the dashed lines depict the classical orbit precessed according to the special relativistic prediction. (c) The same as (b), but with $\eta = 0.3$ (or $\epsilon = 0.550$). (d) The same as (b), but with $\eta = 0.4$ (or $\epsilon = 0.690$).